



## An approach for vegetation mapping and pixel-based change detection for IRS-1C LISS III data

Rubina Parveen<sup>1</sup>, Subhash Kulkarni<sup>2</sup> and V D Mytri<sup>3</sup>

<sup>1</sup>VTU, Belagavi, India

<sup>2</sup>PESIT (South Campus), Bengaluru, India

<sup>3</sup>AIET, Kalaburagi, India

Email: rubina16det@gmail.com

(Received: Jun 08, 2017; in final form: Sep 27, 2017)

**Abstract:** Monitoring and tracking vegetation changes in vast and remote areas is a difficult task. Accurate extraction of existing vegetation is the primary step for better statistical assessment. An approach for vegetation mapping is proposed which automatically explores spectral characteristics of connected components in an image. Different frames of multi-spectral Indian Remote sensing IRS-1C LISS III (Linear Imaging Self-Scanning Sensor) data of different times were used for comprehensive view of vegetation cover. First, quantum of vegetation cover was extracted using band indexing and brightness manipulating techniques for geometrically registered multi-temporal image pair. Secondly, pixel based image differencing method was employed to determine the temporal changes. The accuracy of vegetation extraction was found to be satisfactory by comparing the results with Normalized Difference Vegetation Index vegetation extraction method. Pixel based change analysis technique was assessed statistically by comparison with other change detection techniques like image differencing and band ratioing. Experimental resultant images have demonstrated the efficiency for the proposed approach for the segmentation of vegetation. A statistical value of pixel based change analysis was found to be satisfactory for medium resolution images like IRS-1C LISS III imagery.

**Keywords:** IRS-1C LISS III, spectral response, vegetation mapping, change detection

### 1. Introduction

Natural resource management requires wide knowledge and understanding to identify land cover and associated phenological changes (Verbesselt et al., 2010). Presence of healthy vegetation plays a vital role in environmental changes. Spectral response, resolution and quantitative and qualitative interpretation are the parameters which directly affect the feature extraction from satellite imagery (Parveen et al., 2016). Monitoring vegetation coverage accurately using satellite images and tracking the changes associated with the vegetation coverage is an important task. Many image processing techniques for estimating the fraction of vegetation cover may not function successfully with medium-spatial resolution imagery like the IRS-1C LISS III image (Bannari et al., 2007; Im et al., 2008; Kussul et al., 2012). LISS III data are used for different environmental applications such as dynamics of vegetation cover, wetland assessment, physical characteristics estimation of water bodies and counters and leaf area indexing (Duong, 2012; Zhang and Tian 2015). High-frequency spectral components dominate over minute details of the land cover and results in ambiguity in the target object and background distinction (Pesaresi and Benediktsson, 2001). In this paper, a simple and automatic vegetation mapping segmentation method is proposed followed by change analysis. Here,

vegetation may be agricultural or non-agricultural vegetation but not forest dense vegetation. The proposed algorithm may be considered analogous to spectral segmentation using shadow or dark detection (Khan, 2013; Tsai et al., 2007). However, in contrast to the use of statistical local properties, the proposed approach uses a pixel similarity rule based on the spectral characteristic of similar Geo-technical features in an input image. Spectral characteristics can be compared with reducing topographic effect. Very small frame sample area from the image pairs were selected for analysis, with high spatial uniformity. Comparison can be done by using statistical values of spectral features of vegetation.

Change analysis identifies differences in the state of feature, as same feature has been observed at different times. It quantifies temporal effects, because of repetitive coverage at periodic intervals with unswerving quality of image (Singh, 1989). Various techniques exist in literature for change analysis like automatic threshold (Minu and Shetty, 2015), univariate image differencing (Heikkila and Pietikainen, 2006), image regression (Verbesselt et al., 2010), image ratioing, vegetation index differencing, median filtering-based on background information, principal component analysis, post classification comparison, direct multi-date classification, change

vector analysis, background subtraction (Heikkila and Pietikainen, 2006). The main objective of the study was to identify vegetation, delineation and extraction of vegetation followed by vegetation change mapping using medium resolution multi-spectral and multi-temporal IRS-1C LISS III imagery.

## 2. Data used

Medium spatial resolution IRS-1C LISS III images were used as input data. Study imagery was geometrically registered multi-temporal images belonging to Yadgir district, Karnataka state, India. The location map of study area is shown in Fig. 1. For this study, it is very essential that the multi-temporal data sets be accurately spatially registered. The area is highly heterogeneous in geospatial nature. Small water body, irrigated land, rain fed land and sparse vegetation are seen as major geospatial features. Study area frames are laying around longitude 16 26 49.04 N to and latitude 76 50 02.96 E. A subset of an IRS-1C LISS III scene acquired on April 11, 2006 and October 20, 2006, provided by Karnataka State Remote Sensing Centre, Regional Office Gulbarga, Karnataka state, India, was used. Every pixel covers an area of approximately 552.2 m<sup>2</sup> area. The sensor of LISS-III operates in four different spectral bands. Band 1 is lying between 0.52  $\mu\text{m}$  - 0.59  $\mu\text{m}$  (Green), Band 2 is lying between 0.62  $\mu\text{m}$  - 0.68  $\mu\text{m}$  (Red), Band 3 is lying between 0.77  $\mu\text{m}$  - 0.86  $\mu\text{m}$  NIR (Near Infra-red) and Band 4 is lying between 1.55  $\mu\text{m}$  - 1.70  $\mu\text{m}$  SWIR (Shortwave Infrared-red). Each pixel has 23.5 m resolution. The multi-temporal image of time T1 acquired on April 11, 2006 and image of time T2 acquired on October 20, 2006 are shown in figure 1 (b and c).

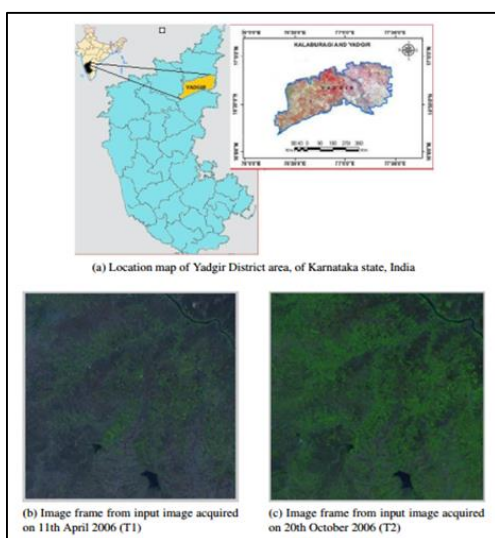


**Figure 1: Input imagery**

## 3. Methodology

The proposed algorithm has been divided into two steps. First step is to extract vegetation by masking all non-vegetation features. Second step is to carry out vegetation change analysis. The image frame of T1 and T2 were first considered for implementation of the algorithm for vegetation extraction, latter processes extended to carry out change analysis. MATLAB 7.10 (R2010a version) image processing tool was used to carry out the analysis. The proposed algorithm is resolution and application specific. The flowchart represents the steps involved in proposed analysis method (shown in Fig. 2).

The following subsections give detailed explanation of the steps involved in methodology.

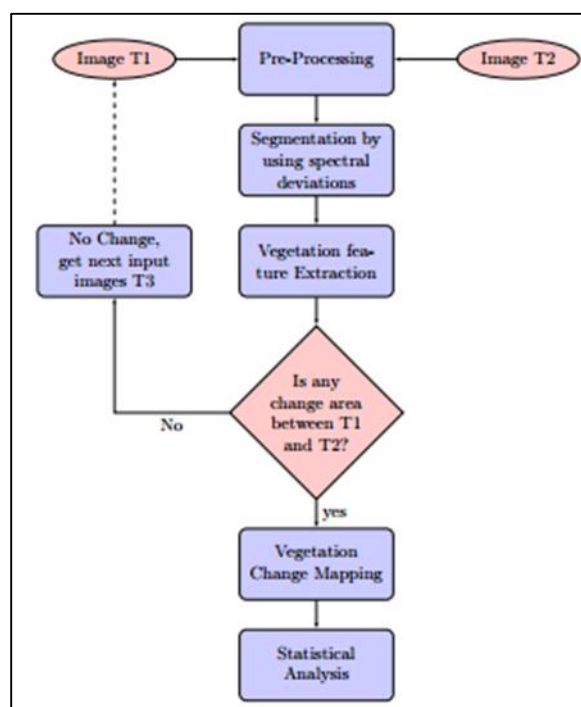


**Figure 2: Flow chart of the proposed methodology**

### 3.1. Pre-processing

Colour of the image pixel, is an instant visual feature Verma et al. (2010) for any analyst. LISS III sensor provides repeatable and consistent measurements at a spatial scale of 23.5 m resolution. It captures effects of natural and man-made processes that cause change (Verbesselt et al., 2010). All the four bands of the input image were analysed separately and the 1st band was found to be not carrying much information. Band 1 is excluded from reducing the redundancy without any loss of vegetation information required for analysis.

Remaining three bands were stacked together to get the one RGB image (Upadhyay and Singh, 2015). Study image (size 7000\*7000 pixels) was represented as 3-D matrix of RGB (Red, Green, and Blue components), resulting in 3D-N dimensional vectors. Due to computational limitations in MATLAB and for visual clarity of lower resolution data, four expedient window frames were extracted from the main frames in MATLAB environment. A subset frame of size 2000\*2000 pixels was taken for the analysis which shows considerable amount of geospatial information required for the study. Four frames were taken for the analysis. First set of extracted frame, as shown in Fig. 1a and Fig. 1b were subjected for histogram equalization (HE).

### 3.2. Segmentation for vegetation extraction

Spectral characteristics of any geo-technical feature will be dominant during the time of acquisition. These spectral features play a vital role in analysis of the image. Spectral characteristics of the image T1 and T2 were observed in band space, (see Fig. 3 a and b).

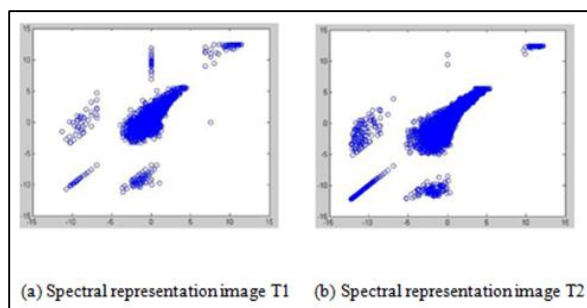


**Figure 3: Spectral responses of imagery**

Pixels were more scattered in Fig. 3a due to mixed presence of vegetation and non-vegetation features. But, pixels were heavily concentrated in -5 to +5 region in Fig. 3b, due to domination of presence of vegetation feature in Image T2. This shows that, the vegetation is more in image T2 than in image T1, because T2 image is acquired in the month of October. In October period more greenery is found than in April. Pixels having similar spectral property were collected as suggested by Tang (2010). Calculation of spectral gradient, brightness manipulation of band ratioing can be done sequentially to extract vegetation pixels. Vegetation indexing always related to leaf area index, vegetation biomass and cropping (Zhang and Tian, 2015). Initially, band ratioing technique is applied to RGB bands of input image, followed by logarithmic operation as shown in Eqn. 1 and Eqn. 2. Band ratioing technique (Bradley et al., 2007) does mathematical transformations of RGB spectral bands that accentuate the spectral properties of vegetation,

distinction between vegetation and non-vegetation pixels. The proposed algorithm does not only differentiate vegetation and non-vegetation pixels more effectively but also detects changes (Tsai et al., 2007). A narrow range of lower intensity pixels values were mapped to a wider range by log transformation. rb and gb are quotient values obtained by band indexing of SWIR and RED bands and NIR and RED bands.

$$rb = \log [SWIR/RED] \quad (1)$$

$$gb = \log [NIR/RED] \quad (2)$$

Two quotient images were generated by simple ratio-based indices (Lyon et al., 1998). Spectral graph shows the amount of vegetation, accentuating the difference between red and NIR reflectance. The darker vegetation pixels of enhanced image were expanded, for better representation. Further, Spatial derivatives, invexp of the bands were calculated by using Eqn. 3 and Eqn. 4.

$$inv = (\cos(rad)*(rb) - \sin(rad)*(gb)) \quad (3)$$

$$invexp = inv * 255 / \max(\max(inv)) \quad (4)$$

Clustering of the spectral gradient, x was done by computing the average of green channel, by using Eqn. 5, gb. Maximum, c1 and minimum c2 integrated images were scaled to match these values to the vegetation pixels. Maximum and minimum of each component was separated and median filtered. For red and green channels, average was calculated by sliding window operation, and the noise was reduced by median filtering. Here, the existence of mixed pixels was considered to be noise.

$$x = (\max(g\_b(:)) + \min(g\_b(:))) / 2 \quad (5)$$

The equation is similar to shadow removing technique of Su et al. (2016), but here vegetation is taken as region of interest. For maximum values of pixels in rb non-vegetation pixels were enhanced and separated by using the Eqn. 6 and Eqn. 7 generating the new spectral values in RG and BG space and thus, which pixels belongs to vegetation was decided.

$$RG(i,j) = inv(i,j) * \cos(-rad) + c1 * \sin(-rad) \quad (6)$$

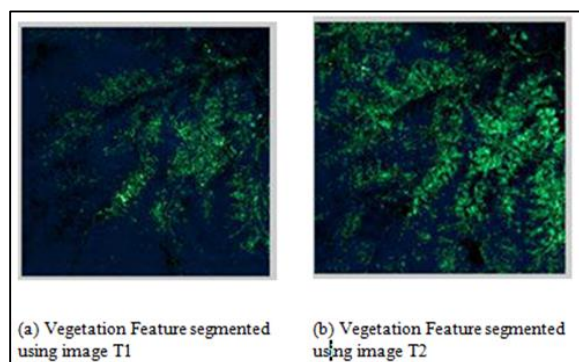
$$BG(i,j) = -inv(i,j) * \sin(-rad) + c1 * \cos(-rad) \quad (7)$$

where, RG (i, j) and BG (i, j) were the newly generated images, after normalization of each pixel value. In RG (i, j) and BG (i, j) images only vegetation pixels were considered for next process. Resulting pixels were

further treated for brightness manipulation to form a new RGB image. Vegetation extracted image from image T1 and T2 are shown in Fig. 4a and 4b. Here it was clearly observed that the vegetation pixels were only highlighted and non-vegetation features were suppressed. Green colored pixels in Fig. 4a and Fig. 4b depict vegetation features.

#### 4. Results and discussion

The quantitative assessment was done based on statistical evaluation. Mean, variance, standard deviation, entropy, energy, homogeneity values and percentage of vegetation occupancy was calculated for both image T1 and T2. Results are tabulated in Table 1.



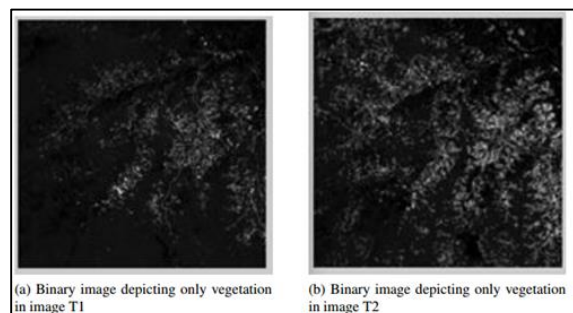
**Figure 4: Vegetation extracted imagery**

Fig. 4a and b were converted into gray scale and subjected to intensity thresholds by determining threshold. Pixel intensity higher than threshold was set to white in the output and pixel's intensity lower than threshold were set to black in the output. Resultant binary image maps only clear vegetation pixels, as shown in Fig. 5a and b. Black pixels correspond to non-vegetated areas and white pixel correspond to vegetation areas. Non-zero pixels were calculated to determine the occupancy of these pixels in the entire image by using the Eqn. 8.

$$\text{PercentageOccupancy} = \left( \frac{\sum(\text{rgb}(i, j))}{\sum(I(i, j))} \right) * 100 \quad (8)$$

**Table 1: Statistical analysis for multi-temporal IRS-1C LISS III imagery**

Sl. No.	Images of time T1	Images of time T2	Analysis
Number of Vegetation Pixels	5916	12685	Vegetation Pixels in T1 is less than vegetation pixels in T2
Percentage Occupancy of vegetation	4.95	10.63	Difference is 5.67
Mean	0.0042	0.197	Arithmetic average values are more in T2
Variance	0.0014	0.0066	spread of vegetation pixel distribution around the mean is more in T2
Standard Deviation	0.0264	0.0517	Shows how spread out the pixels are
Entropy	0.0388	0.14	complexity of texture in T2 because of more
Energy	0.0476	0.0601	texture uniformity appears to be more constant for image T2
Homogeneity	0.0047	0.3428	most of the elements in T2 are same



**Figure 5: Segmented binary imagery**

In image T1, 5916 vegetation pixels exists with 4.95 percentage of vegetation occupancy and in image T2 12685 vegetation pixels exists with 10.63 percentage of vegetation occupancy. Same input image frames were subjected to Normalized Difference Vegetation Index (NDVI) technique (Verbesselt et al., 2010) using Eqn. 9 to identify the vegetation cover.

$$\text{NDVI} = (\rho_{\text{NIR}} - \rho_{\text{red}}) / (\rho_{\text{NIR}} + \rho_{\text{red}}) \quad (9)$$

where,  $\rho_{\text{NIR}}$  and  $\rho_{\text{red}}$  are reflectance in NIR and RED bands. NDVI uses spectral properties of LISS III image bands. Normalization balances the effects of non-uniform illumination. Normalization can be addressed by performing an atmospheric correction of each image, by considering reflectance of invariant targets. NDVI is normally calculated by applying simple user defined threshold. For automatic vegetation extraction by NDVI, results in the study were taken without any applying threshold. From the results of the NDVI, vegetation cover in image frame T1 is 40.18 percentage and vegetation cover in image frame T2 is 44.62 percentage. NDVI technique segmented images are shown in Fig. 6a for frame T1 and Fig. 6b for frame T2.

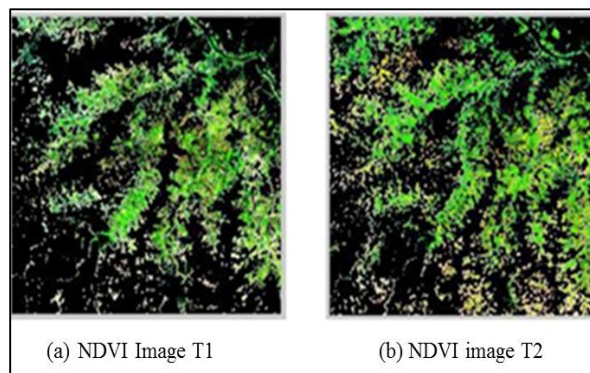


**Figure 6: Normalize Difference Vegetation Index (NDVI) imagery**

Percentage of vegetation occupancy in NDVI is more than proposed algorithm. It was observed that NDVI segmented image does not show sharp vegetation boundaries. NDVI image shows the presence of noise as mixed pixels and pixels other than green colour. The result of NDVI was visually not clear as compared to proposed algorithm.

Vegetation change analysis using satellite images has been widely investigated (Cheng et al., 2004) for greenery monitoring. Unsupervised type (Bruzzone and Prieto, 2000) of change analysis was employed Singh (1989). Vegetation change detection study was focused on correlation analysis (Alesheikh et al., 2007) using multi-temporal imagery. Brightness values of multi-temporal image data-sets, was compared to extract uncorrelated pixels (Im et al., 2008). Common properties of the pixels were identified. Pixel based change detection technique was employed in the study by using Eqn. 10. This algorithm calculates the absolute difference between multi-temporal imagery automatically (Misra et al., 2012).

$$\text{rgb}(i,j)_d = \text{imabsdiff}(\text{rgbT1}(i,j), \text{rgbT2}(i,j)) \quad (10)$$

where,  $\text{rgbT1}(i,j)$  and  $\text{rgbT2}(i,j)$  vegetation extracted imagery.  $\text{rgb}(i, j)_d$  is the resultant image (Fig.7a) highlights changes between T1 and T2 images. A 6.9 percentage of vegetation change is obtained by Eqn. 10.

Change magnitude was generated by using correlation between multi-temporal and multi-spectral LISS III data sets (Im et al., 2008). Pixel based change detection as shown in Fig. 7a appears to be visually clear with 6.9 percentage positive changes. This value is compared with image difference based change analysis (Fig. 7b) with 8.9 percentage changes and band ratio based change analysis (Fig. 7c), with 33.5 percentage changes. Percentage of occupancy of vegetation in T1 and T2 is 4.9 and 10.6 percentage. Simple numerical difference is 5.67 percentage and pixel based change detection gives 6.9 percentage of change. Thus proposed algorithm achieves 83.6 percentage accuracy. The algorithm has been tested on next set of multi-temporal three frames extracted from input frames. Fig. 8 shows results of second testing set of frames. Fig. 9 shows results of third testing set of frames. Fig. 10 shows results of fourth testing set of frames.

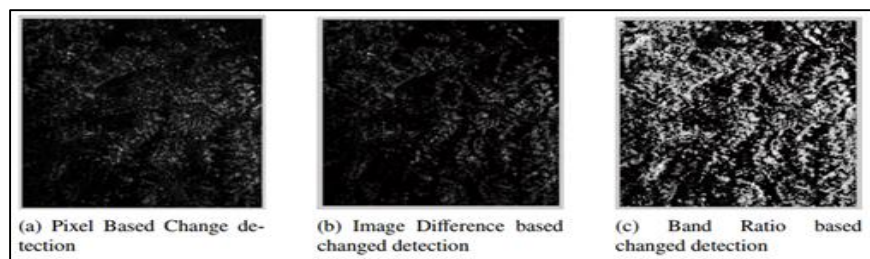


**Figure 7: Vegetation extracted imagery**

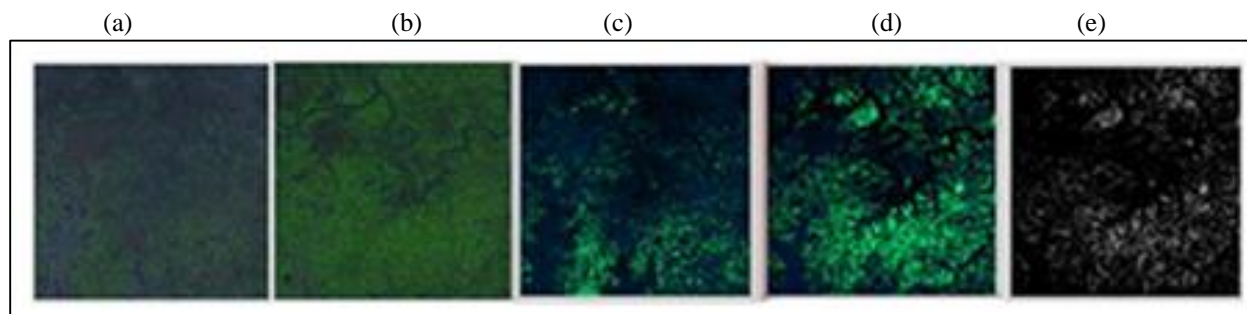


**Figure 8: Second frame analysis (a) T1 image; (b) T2 image; (c) Vegetation extracted from T1 image; (d) Vegetation extracted from T2 image; and (e) change mapped image**

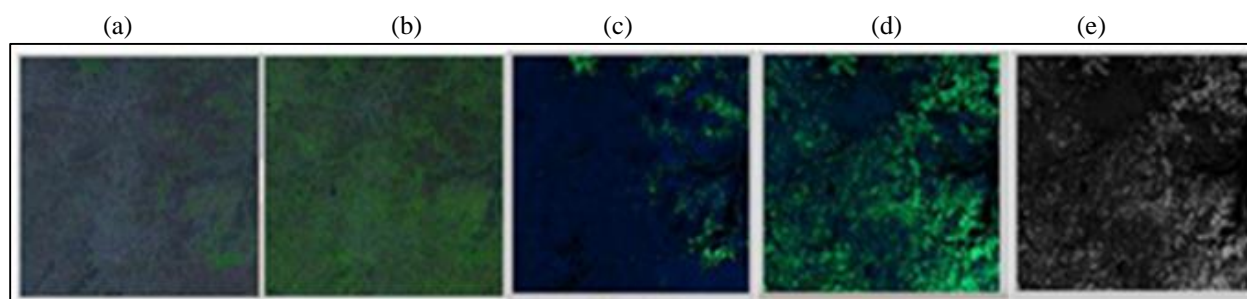


**Figure 9: Third frame analysis (a) T1 image; (b) T2 image; (c) Vegetation extracted from T1 image; (d) Vegetation extracted from T2 image; and (e) change mapped image**

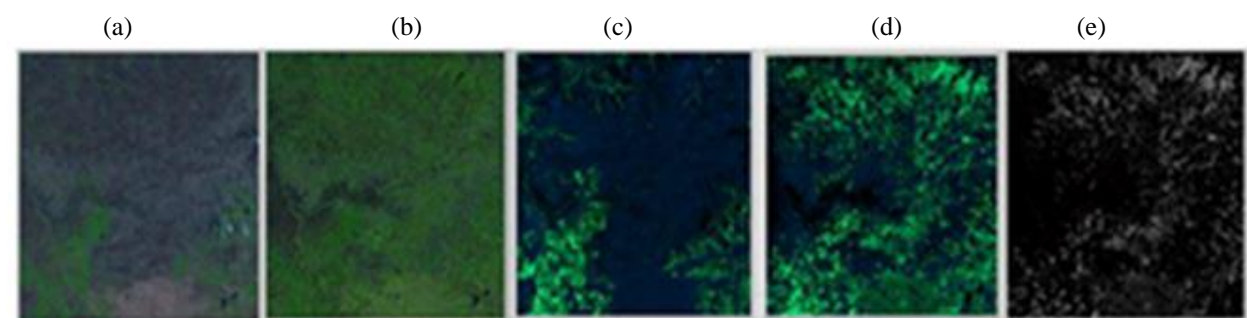


**Figure 10: Fourth frame analysis (a) T1 image; (b) T2 image; (c) Vegetation extracted from T1 image; (d) Vegetation extracted from T2 image; and (e) change mapped image**

**Table 2: Statistical analysis for multi-temporal IRS-1C LISS III imagery**

Frame numbers	Percentage of vegetation in T1 image	Percentage of vegetation in T2 image	Simple Arithmetic Subtraction	percentage change map	Comparison
First frame	4.95	10.63	5.76	6.7	1.06 percentage more vegetation was detected
Second frame	5.98	12.52	6.54	7.85	1.31 percentage more vegetation was detected
Third frame	2.37	11.48	9.11	8.49	0.6 percentage less vegetation was detected
Fourth frame	5.43	13.2	7.77	8.49	0.72 percentage less vegetation was detected

The performance of algorithm on four frame data sets are reported in Table 2. Very clear vegetation features were extracted and change map has been carried out to determine the seasonal changes (Kussul et al., 2012). Frames one and two show positive changes whereas, frames 3 and 4 show negative changes.

Overarching goal of the proposed work was to develop a simple method for vegetation extraction and change mapping vegetation areas using multi-temporal image of a medium resolution imagery like IRS-1C LISS III image. Vegetation area statistics were generated and compared with NDVI statistics. Features extracted from the algorithm can be used to get spatial information like shape, texture, hierarchy and spectral information. The proposed algorithm is automatic and simple to implement. This information can be used for application specific work. Pixel based change detection is simple and fast for computation by automatically correlating and comparing multi-temporal LISS III data set, taken of the same area, at different times. The resultant images display the positive and negative changes at respective locations. Repetition of the assessment was done by evaluating the results on various testing data sets. Quantitative results were found to be satisfactory and visually clear. Accuracy of this pixel based change detection critically depends upon the accuracy of geometric registration of multi-temporal imagery. Exact geometric registration of data depends on accurate ground control points. Further, study has to be carried out to develop more generic change detection techniques which work accurately even with non-geometrically registered images and cloud covered images. The algorithm can be extended to characterize and label the changes. However, the results of the proposed work have limitation because of a number of short period multi-temporal data sets. Succeeding

sections deals with the data set and software tools used for the implementation of the algorithms.

## 5. Conclusion

The study proposes a simple automatic methodology to identify vegetation, delineation and extraction of vegetation followed by vegetation change mapping using medium resolution multi-spectral and multi-temporal IRS-1C LISS III imagery. The validation of results was carried out by comparing change map values with other techniques like image ratioing technique. Proposed algorithm was found to be a very good tool for vegetation feature extraction and change detections.

## References

- Alesheikh, A.A., A. Ghorbanali and N. Nouri (2007). Coastline change detection using remote sensing. *International Journal of Environmental Science & Technology*, vol. 4, no. 1, 61–66.
- Bannari, A., A. Ozbaldr and A. Langlois (2007). Spatial distribution mapping of vegetation cover in urban environment using TDVI for quality of life monitoring. *IEEE International Geoscience and Remote Sensing Symposium*, 679–682.
- Bradley, D.M., R. Unnikrishnan and J. Bagnell (2007). Vegetation detection for driving in complex environments. *Proceedings of the 2007 IEEE International Conference on Robotics and Automation*, 503–508.
- Bruzzone, L. and D.F. Prieto (2000). Automatic analysis of the difference image for unsupervised

- change detection. *IEEE Transactions on Geoscience and Remote sensing*, vol. 38, no. 3, 1171–1182.
- Cheng, K., C. Wei and S. Chang (2004). Locating landslides using multi-temporal satellite images. *Advances in Space Research*, vol. 33, no. 3, 296–301.
- Duong, N.D. (2012). Water body extraction from multi spectral image by spectral pattern analysis. *International Archives of the Photogrammetry, Remote Sensing and Spatial Information Sciences*, vol. 39, B8.
- Heikkila, M. and M. Pietikainen (2006). A texture-based method for modelling the background and detecting moving objects. *IEEE transactions on pattern analysis and machine intelligence*, vol. 28, no. 4, 657– 662.
- Im, J., J. Jensen and J. Tullis (2008). Object-based change detection using correlation image analysis and image segmentation. *International Journal of Remote Sensing*, vol. 29, no. 2, 399–423.
- Kussul, N., S. Skakun, A. Shelestov, O. Kravchenko, J. F. Gallego and O. Kussul (2012). Crop area estimation in Ukraine using satellite data within the mars project. *IEEE International Geoscience and Remote Sensing Symposium*, 3756–3759.
- Khan, W. (2013). Image segmentation techniques: A survey. *Journal of Image and Graphics*, vol. 1, no. 4, 66–170.
- Lyon, J.G., D. Yuan, R.S. Lunetta and C.D. Elvidge (1998). A change detection experiment using vegetation indices. *Photogrammetric engineering and remote sensing*, vol. 64, no. 2, 143–150.
- Minu, S. and A. Shetty (2015). A comparative study of image change detection algorithms in Matlab. *Aquatic Procedia*, vol. 4, 1366–1373.
- Misra, G. A. Kumar, N. Patel, R. Zurita-Milla and A. Singh (2012). Mapping specific crop - A multi sensor temporal approach. *IEEE International Geoscience and Remote Sensing Symposium*, 3034–3037.
- Parveen, R., S. Kulkarni and V. Mytri (2016). Vegetation extraction from multi sensor IRS-1C LISS III image by principle component analysis and comparative assessment. *2nd International Conference on Advances in Electrical, Electronics, Information, Communication and Bio-Informatics (AEEICB)*, 2016, 368–372.
- Pesaresi, M. and J.A. Benediktsson (2001). A new approach for the morphological segmentation of high-resolution satellite imagery. *IEEE transactions on Geoscience and Remote Sensing*, vol. 39, no. 2, 309–320.
- Singh, A. (1989). Digital change detection techniques using remotely-sensed data. *International journal of remote sensing*, vol. 10, no. 6, 989–1003.
- Su, N., Y. Zhang, S. Tian, Y. Yan and X. Miao (2016). Shadow detection and removal for occluded object information recovery in urban high-resolution panchromatic satellite images. *IEEE Journal of Selected Topics in Applied Earth Observations and Remote Sensing*, vol. 9, no. 6, 2568–2582.
- Tsai, F. E.-K. Lin and K. Yoshino (2007). Spectrally segmented principal component analysis of hyperspectral imagery for mapping invasive plant species. *International Journal of Remote Sensing*, vol. 28, no. 5, 1023-1039.
- Tang, J. (2010). A color image segmentation algorithm based on region growing. *2nd International Conference on Computer Engineering and Technology (ICCET)*, vol. 6, V6–634.
- Upadhyay, A. and S.K. Singh (2015). Classification of IRS LISS III images using PNN. *Proceedings of the 2nd International Conference on Computing for Sustainable Global Development (INDIACom)*, 2015, 416–420.
- Verbesselt, J., R. Hyndman, G. Newnham and D. Culvenor (2010). Detecting trend and seasonal changes in satellite image time series. *Remote sensing of Environment*, vol. 114, no. 1, 106–115.
- Verma, D., N. Garg, N. Garg, N. Mishra and G. Dosi (2010). Development of descriptors for natural feature identification on IRS LISS-III images. *Proceedings of the International Conference on Methods and Models in Computer Science (ICM2CS)*, 2010, 54–58.
- Zhang, X. and Q. Tian (2015). Comparison of spectral characteristics between EO-1 ALI and IRS-P6 LISS-III imagery. *Current Science*, vol. 108, no. 5, 954 – 960.